Proc. Natl. Acad. Sci. USA
Vol. 87, pp. 7603–7607, October 1990
Biophysics

Direct detection of linker DNA bending in defined-length oligomers of chromatin

J. YAO*†, P. T. LOWARY*‡, AND J. WIDOM*†‡§¶

Departments of *Chemistry, ‡Biochemistry, and §Biophysics, and †Beckman Institute, University of Illinois at Urbana–Champaign, Urbana, IL 61801

Communicated by Donald M. Crothers, July 9, 1990

ABSTRACT **Linker DNA, which connects between nucleosomes in chromatin, is short and, therefore, may be essentially straight and inflexible. We have carried out hydrodynamic and electron microscopic studies of dinucleosomes—fragments of chromatin containing just two nucleosomes—to test the ability of linker DNA to bend. We find that ionic conditions that stabilize the folding of long chromatin cause linker DNA in dinucleosomes to bend, bringing the two nucleosomes into contact. The results uphold a key prediction of the solenoid model of chromosome folding and suggest a mechanism by which proteins that are separated along the DNA can interact by direct contact.**

Eukaryotic chromosomes are maintained throughout much of the cell cycle in an intermediate level of folding in which a chain of nucleosomes is compacted into a 30-nm-wide filament (1, 2). A widely held model of the structure of 30-nm filaments, the solenoid model (3–5), requires the DNA connecting between nucleosomes (linker DNA) to have an unexpected property: it must bend to bring consecutive nucleosomes into direct contact (2).

The mechanical properties of naked DNA can be predicted by comparing the DNA length with a length scale for polymer stiffness, known as the persistence length (6). For DNA, the persistence length decreases as the $[Na^+]$ is increased, reaching a limiting (smallest) value of ≈50 nm [150 base pairs (bp)] for $[Na^+] > 10$ mM (6, 7). The length of linker DNA is variable, typically within the range ≈0 to ≈80 bp (1); for chicken erythrocyte chromatin used in the present study, the linker DNA is ≈45 bp (≈15 nm) in average length. Linker DNA is thus short compared even to the limiting persistence length.

The effect of thermal fluctuations on short DNA molecules is to cause small random local bends in uncorrelated directions along the DNA length. This in turn reduces the average end-to-end separation of the DNA from the value that would obtain if the DNA were not flexible. The worm-like coil model allows one to calculate the expected rms end-to-end separation (R) (6). For chicken erythrocyte chromatin, the average linker DNA length (L) is 1/3.3 times the limiting persistence length, leading to $R = 0.95\ L$. The average end-to-end separation of the DNA is 5% less than the contour length. Thus, if the properties of linker DNA are those of naked DNA, the linkers will be on average nearly fully extended. This picture is in accord with the known behavior of chromatin. In dilute Na^+ solutions, 30-nm filaments unfold and adopt an extended conformation in which the linker DNA does take an approximately straight path from one nucleosome to the next (2).

Alternative "cross-linker" models of 30-nm filaments have been proposed (8–10) that are outwardly similar to the solenoid model but have a different connectivity and allow the linker DNA to remain straight. When chromatin folds into 30-nm filaments, does the linker DNA remain straight or does it bend? The answer to this question is important also because it determines whether two proteins that are separated from each other along the same or nearby linker regions will be in close three-dimensional proximity. In the present report, we focus on dinucleosomes—defined-length oligomers of chromatin containing just two nucleosomes and one linker—to study the bendability of linker DNA. Dinucleosomes allow the unambiguous detection of linker DNA bending through measurement of their nucleosome–nucleosome distance.

MATERIALS AND METHODS

Dinucleosomes were purified from random short fragments of chicken erythrocyte chromatin (11), as described by Butler and Thomas (12).

Electron micrographs were obtained using the alcian blue method of Sogo and Thoma (13). Dinucleosomes were dialyzed into 2 mM sodium phosphate (pH 7.5, supplemented with additional salts when desired), glutaraldehyde was added to 0.1% by dialysis, and the dinucleosomes were fixed overnight at 4°C. The samples were then dialyzed into buffer without additional salts, adsorbed to alcian blue-treated carbon films, washed extensively with deionized H_2O, dried in ethanol, and shadowed with platinum. A negatively stained catalase crystal was used as a magnification standard.

The dynamic light scattering data were obtained with a commercial instrument consisting of a Brookhaven Instruments (Holtsville, NY) BI-2030 autocorrelator and BI-200 goniometer and a Coherent Radiation (Palo Alto, CA) Innova-90 argon ion laser. The laser was operated at 488 nm with up to 300 mW of power. Measurements were made at 21 or 23°C. Samples were centrifuged to remove dust prior to measurement.

RESULTS AND DISCUSSION

Biochemical Characterization of Dinucleosomes. The distribution of DNA lengths in the purified dinucleosomes is illustrated in Fig. 1*a*. The average DNA length is 420 bp, as expected for a dimer of 210-bp-containing dinucleosomes (1). It is important to determine the stoichiometry of histone H1 (and its variant, H5) in the purified dinucleosomes, because they are easily lost from short oligonucleosomes (14, 15). The protein composition of the purified dinucleosomes is shown in Fig. 1*b*, compared to that of long chromatin in Fig. 1*c*. From the relative peak areas for H1 plus H5 and H4 in the two samples, we calculate that the purified dinucleosomes have lost roughly 15% of the H1 plus H5. The stoichiometry of H1 plus H5 in native chicken erythrocyte chromatin is 1.3 molecules per nucleosome (16), so the stoichiometry in the purified dinucleosomes is 1.1 molecules of H1 plus H5 per nucleosome.

The publication costs of this article were defrayed in part by page charge payment. This article must therefore be hereby marked "*advertisement*" in accordance with 18 U.S.C. §1734 solely to indicate this fact.

¶To whom reprint requests should be addressed at: Department of Chemistry, University of Illinois, Urbana, 505 South Mathews Avenue, Urbana, IL 61801.

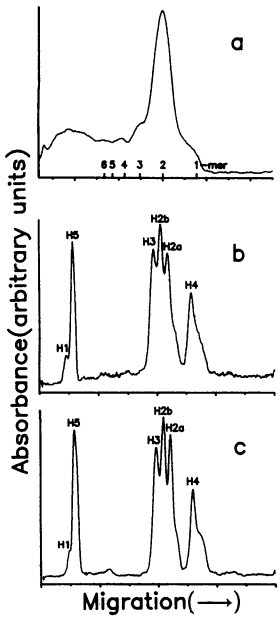

FIG. 1. (*a*) Densitometer tracing of a photograph of DNA present in purified dinucleosomes from a 2% agarose gel with ethidium stain. The positions of mononucleosomes and higher oligomers (determined from densitometer tracings of gel tracks from other sucrose gradient fractions) are marked. *Hae* II restriction fragments of pBR322 were used as length markers. (*b* and *c*) Densitometer tracing of Coomassie blue-stained 18% polyacrylamide gel of proteins present in the purified dinucleosomes and in long (native) chromatin, respectively.

Dynamic Light Scattering Studies. *In vitro*, titrating long chromatin with cations causes it to fold progressively into the 30-nm filament state (2). We tested for a Na^+-dependent compaction of the dinucleosomes by using dynamic light scattering to measure translational diffusion coefficients (D_t). The results are shown in Fig. 2. From 1 mM Na^+ (when long chromatin is known to exist in the extended nucleosome filament conformation) to 18 mM (when long chromatin has begun to visibly compact), the diffusion coefficient of dinucleosomes increases by 16%. The sign of the change in D_t plus the insensitivity of the results to the concentration of dinucleosomes argue against charge effects or other artifacts as possible explanations for the results (17). The absence of any abrupt change in D_t near 1 mM Na^+ shows that the results are

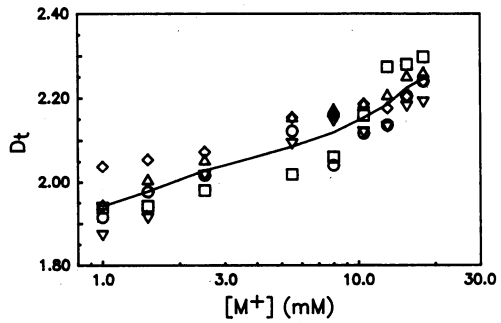

FIG. 2. D_t of dinucleosomes in various Na^+ concentrations at 23°C. Dinucleosomes were dialyzed against a buffer containing 1 mM Tris·HCl (pH 7.5) and 0.1 mM $Na_{2.5}$EDTA and then mixed with an equal volume of buffer plus NaCl. ◇, 0.085 mg/ml (preparation 3); ▽, 0.090 mg/ml (preparation 2); △, 0.088 mg/ml (preparation 1); □, 0.036 mg/ml (preparation 2); ○, 0.035 mg/ml (preparation 1). Each symbol represents an average of at least three measurements; for each sample, the reproducibility was ±3% or better. The solid line represents an average over the five separate experiments. Values of D_t are expressed as cm^2/sec ($\times 10^7$).

not affected by nucleosome unfolding, which can occur if H1 or H5 are not present (18, 19). Thus, the increase in D_t means that the dinucleosomes are becoming more compact. Continuation of the titrations to higher [Na^+] led to aggregation of the dinucleosomes, as judged by an increase in the total intensity of light scattering and an accompanying decrease in the apparent diffusion coefficient (data not shown); the onset of aggregation occurs in the range of 25–35 mM Na^+. In such conditions it is no longer possible to measure D_t. We, therefore, consider only the data for [Na^+] < 20 mM. Up to this point, the data in Fig. 2 show no signs of reaching a plateau. We conclude that the compaction is not complete in 20 mM Na^+.

Previous hydrodynamic studies had reported that dinucleosomes showed no detectable [Na^+]-dependent compaction (12, 20, 21). However, those studies were focused chiefly on longer oligomers; short oligomers were less thoroughly studied. Also, most of the previous studies (1, 12, 21) were of rat liver chromatin. Long chicken erythrocyte chromatin is known to form compact structures that are more stable than those from rat liver chromatin (22); possibly this difference applies also to dinucleosomes.

One mechanism that could lead to the observed compaction is a Na^+-dependent sliding together of the two histone octamers along the DNA (for review, see ref. 1). However, four lines of evidence argue against this possibility. Octamers are not able to slide when histone H1 is present. Even in the absence of H1, octamer sliding generally requires long times at elevated temperatures and ionic strengths—conditions that are not approached in the present study. If sliding were able to take place, it should have happened during the preparative nuclease digestion. This would lead to dinucleosomes having shorter DNA lengths than the 420 bp that we observe. Finally, the sliding apart of H1-depleted octamers that have slid together has never been demonstrated; yet, given the manner in which our dinucleosomes are prepared, the compaction observed in this study must be reversible.

There remain two mechanisms that could lead to dinucleosomes becoming more compact: groups on each nucleosome (e.g., the "tails" of the core histones or of H5) could be extended into the solvent in 1 mM Na^+ but could retract when the [Na^+] is increased, or the linker DNA could bend to bring the two nucleosomes together in space. These two mechanisms can be distinguished by hydrodynamic studies of monomer particles such as chromatosomes or nucleosome core particles. Numerous such studies have been carried out (for review, see ref. 1). Over the range in [Na^+] used in the present study, nucleosome core particles and chromatosomes show an increase in sedimentation coefficient (S) (which is equivalent to D_t) of 5% or less (18, 19, 23). Our own measurements of D_t for nucleosome core particles over the range 3 mM to 28 mM monovalent cation (M^+) are given in Table 1. These data are consistent with an increase of less than 3% in D_t. We conclude that the observed increase in D_t for dinucleosomes is due to a mode of Na^+-dependent compaction that is unavailable to mononucleosomes: the linker DNA bends to bring the two nucleosomes toward contact.

Table 1. D_t of nucleosome core particles

M^+, mM	D_t, cm^2/sec ($\times 10^7$)
3	3.98 ± 0.08
13	4.07 ± 0.03
28	4.05 ± 0.01
Average	4.03 ± 0.09

Data were obtained at 21°C with core particles at 0.1–0.5 mg/ml, dialyzed into 5 mM Tris·HCl, pH 7.5/1 mM benzamidine/0.1 mM EDTA, plus 0, 10, or 25 mM NaCl, corresponding to 3, 13, or 28 mM M^+, respectively.

One can also compare our actual measured values for D_t with the results from other studies, such as the data in Table 2. Data for chicken erythrocyte dinucleosomes are available for $[M^+] \approx 10$ mM (24). Our results for this $[M^+]$ agree with those reported (24), and both agree with the expected value for D_t calculated from the dinucleosome's sedimentation coefficient that was reported in the same study. One study of rat liver dinucleosomes (21) reports a $[Na^+]$-independent value of D_t of 2.25×10^{-7} cm^2/sec, which is also in reasonable agreement. Our measurements of D_t for core particles agree with the D_t calculated from the measured sedimentation coefficient, for which there are numerous good data (1, 18, 23). Our measurements also agree with a result obtained from a sedimentation velocity experiment using the boundary-spreading method, $D_t \approx 3.90 \times 10^{-7}$ cm^2/sec (25). Three other studies are not strictly comparable. Two of these (21, 26) report data for mononucleosomes, which include extra DNA and histone H1. A third study (27) reports dynamic light-scattering data for nucleosome core particles; but this was carried out under conditions of limiting $[M^+]$ (i.e., not dialysis equilibrium), which is known to lead to an increase in frictional coefficient (23).

Hydrodynamic Simulations. To relate the observed magnitude of the increase in D_t for the dinucleosomes to an extent of compaction, we carried out computer simulations for a simple model (Fig. 3). The dinucleosomes were represented as two disks, each having a diameter of 11 nm and a thickness of 6 nm, and the bending of linker DNA was simulated by varying the distance between them. Since there is no information available regarding the hydrodynamic properties of the histone "tails" or of linker DNA, these were omitted from the calculations. The average linker DNA length for chicken erythrocyte chromatin is 45 bp or 15 nm. When two disks, initially separated by a distance of 15 nm (models I and IV), are brought together side to side (models II and V), D_t increases by 21%; if the two disks are brought together face to face (model III), D_t increases by 41%. We conclude that the measured increase in D_t can be accounted for by a Na^+-dependent approach of the two nucleosomes toward contact. The data are consistent with any of the limiting structures (models II, III, and V). We cannot distinguish between these models with our experimental data, since we do not reach a titration end point.

Electron Microscopy. We have tested the conclusion derived from the hydrodynamic experiments by directly imaging dinucleosomes in the electron microscope. To avoid preparative artifacts, samples were equilibrated in various ionic conditions, fixed, then dialyzed into a common low-$[Na^+]$ adsorption buffer, and prepared for microscopy without the use of heavy metal stain (4). Fig. 4 *a–c* shows micrographs obtained for chromatin in 2 mM Na^+, 20 mM Na^+, and 2 mM Mg^{2+} [a condition in which the 30-nm filament state is fully formed (2)], respectively. (Dinucleosomes in 2 mM Mg^{2+} aggregate at the relatively high concentrations required for dynamic light scattering, but the electron micrographs are obtained from much more dilute samples where aggregation appears not to be a problem.) The images suggest that the dinucleosomes in 20 mM Na^+ and in 2 mM Mg^{2+} are more compact than those in 2 mM Na^+.

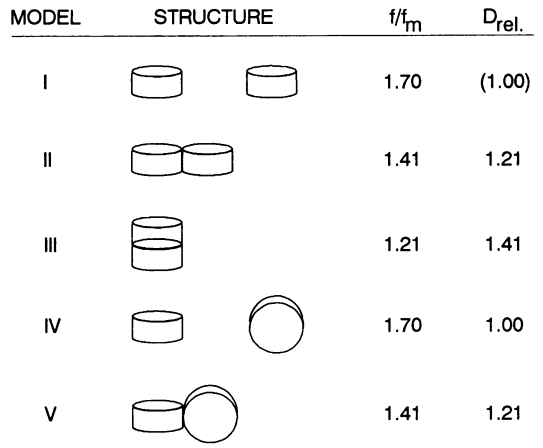

FIG. 3. Hydrodynamic simulations. Each disk was represented by 616 small spheres on a cubic lattice. The radius of the small spheres was chosen so as to make their aggregate volume equal to that of the two disks. Frictional coefficients were calculated for a single (isolated) disk and for the pairs of disks illustrated by using standard methods (28). The results are presented as frictional ratios f/f_m, in which the frictional coefficient for each pair of disks (f) is divided by that for a single disk (f_m). D_t is proportional to $1/(f/f_m)$; relative values (D_{rel}) are given here, with the value for model I set to 1.00.

The images were quantitated objectively by measuring the widths (i.e., long axis) of every dinucleosome present, on enlarged prints of the micrographs. Histograms of the widths are shown in Fig. 5 *a–c*. Dinucleosomes in 20 mM Na^+ and in 2 mM Mg^{2+} are indeed more compact than those in 2 mM Na^+.

The width (diameter) of single nucleosomes in the dinucleosomes was also measured from the prints and yielded an average diameter of 15.7 nm (taking into account the known magnification), independent of the ionic conditions. Nucleosomes are known to be 11 nm in diameter (29); they are evidently enlarged by shadowing. The center-to-center internucleosomal distance in dinucleosomes should be independent of the shadowing. It can be determined by subtracting the measured nucleosome diameter from the measured width of the dinucleosomes. Also shown in Fig. 5 *d* and *e* are difference histograms in which the normalized width distribution for 2 mM Na^+ was subtracted from the normalized distribution for 20 mM Na^+ or for 2 mM Mg^{2+}, respectively,

Table 2. Comparison of S and D_t

Sample	M^+, mM	S_{meas}, S	D_{calc},* cm^2/sec ($\times 10^7$)	D_{meas}, cm^2/sec ($\times 10^7$)
Nucleosome core particles	2–30	10.8–11.1†	3.84–3.95	4.03 ± 0.09‡
				3.90 ± 0.13§
Dinucleosomes	≈10	16.2¶	2.19	2.15 ± 0.04‡
				2.16 ± 0.10¶

*Calculated for $D = [RT/M(1 - \bar{v}\rho)]\,S$, with $\bar{v} = 0.663$ (ref. 23) and with M(core particle) = 204,000 and M(dinucleosome) = 534,000, and where D is the diffusion coefficient, M is the molecular weight in daltons, $\bar{v}$ is the partial specific volume of the nucleosome core particle in cm^3/g, ρ is the solvent density in g/cm^3, and S is the sedimentation coefficient.
†Data are from refs. 18, 23.
‡This study.
§Data are from ref. 25.
¶Data are from ref. 24.

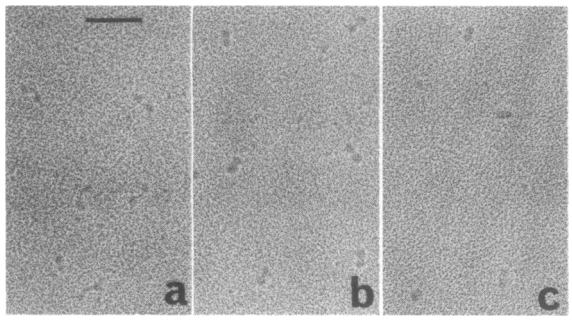

FIG. 4. Electron micrographs of dinucleosomes in 2 mM sodium phosphate (pH 7.5) (*a*), buffer plus 18 mM Na^+ (*b*), or buffer plus 2 mM Mg^{2+} (*c*). (Bar = 100 nm.)

and plotted as a function of the dinucleosome center-to-center distance.

The mode of the internucleosomal distance distributions is 26 nm for dinucleosomes in 2 mM Na^+, and 12 nm for dinucleosomes in 20 mM Na^+ or in 2 mM Mg^{2+}. By assuming that the nucleosomes preferentially lie with their flat faces on the carbon surface (4), a dinucleosome center-to-center distance of 26 nm corresponds to an edge-to-edge separation of 15 nm, which is the distance expected if the linker DNA were extended in 2 mM Na^+. The center-to-center distance of 12 nm obtained for 20 mM Na^+ and for 2 mM Mg^{2+} corresponds to an edge-to-edge separation of only 1 nm; in these conditions, the two nucleosomes of most dinucleosomes are almost touching.

CONCLUSIONS

The results from this study show that linker DNA can bend to bring two consecutive nucleosomes into contact. This unexpected finding upholds a key prediction of the solenoid model of chromatin folding. One question that arises is whether the observed ability of the linkers to bend is typical of all linkers in a long chain or is unique to the chain ends. In a previous study (30), short oligonucleosomes were examined in uranyl acetate with dilute Na^+ and were found by electron microscopy often to have their nucleosomes in contact. The status of that work became uncertain when it was discovered in solution studies that, in dilute Na^+, linker DNA is actually extended and nucleosomes are not in contact (2). Our results suggest that the uranyl acetate may have facilitated the observed compaction. In that study (30), tetranucleosomes were observed in which all four nucleosomes were in contact. Although one cannot identify which two nucleosomes are internal, the internal linkers must nevertheless have been bent. The ability of a linker to bend may not depend on its proximity to an end.

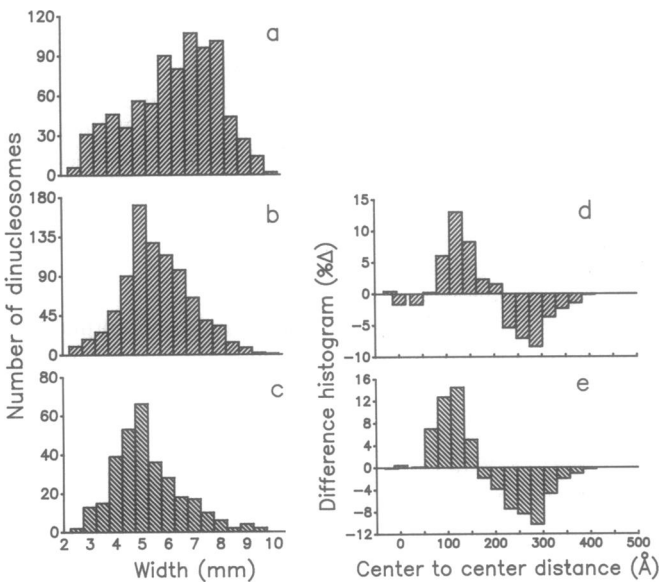

FIG. 5. (*a–c*) Histograms of widths of dinucleosomes, measured from prints at ×180,000 magnification. Conditions in *a–c* correspond to those as described in Fig. 4 *a–c*, respectively. (*d* and *e*) Difference histograms, plotted as a function of the center to center internucleosomal distance (see text). The histograms in *a–c* were normalized (integrals scaled to 100%) and then subtracted in pairs. (*d*) Histogram values in *b* minus histogram values in *a*. (*e*) Histogram values in *c* minus histogram values in *a*.

A separate question is whether linkers do bend when long chromatin folds. The present results suggest that there is a natural tendency in chromatin for consecutive nucleosomes to pack together, bending the linker DNA that connects them; but it is possible that the actual behavior of long oligomers could differ from that of short ones, because of interactions that might exist only for oligomers greater than some critical length. If such effects were insignificant, the present results would cast doubt on crossed linker models of the 30-nm filament (8–10) in which linker DNA is required to remain straight. Two significant consequences of linker DNA bending in chromatin are that consecutive nucleosomes along the DNA will be in contact in the higher order structure and that two proteins on the same or adjacent linker regions may be neighbors in three-dimensional space.

What is the mechanism of linker DNA bending? The bending is cation-induced and thus is not due to sequence-specific fixed curvature. Linker DNA appears to be random in sequence, although it appears to be enriched in nearest neighbor sequences having a lower than average thermal stability (31). Although such sequences have been termed "flexi-DNA," this refers to a propensity to unwind preferentially under the influence of negative torsional strain (31). Both nucleosomes of our dinucleosomes are expected to be able to rotate independently and, therefore, the linkers should not be subject to significant torsional strain. There is no firm evidence at this time for a sequence dependence to the bending flexibility of DNA (6). Moreover, even if linker DNA had an extraordinarily low persistence length of only ≈45 bp (for which there is no precedent), so that the average linker DNA length was on the order of one persistence length, the rms end-to-end separation for the linker DNA would still be 86% of the contour length (6). Such a small change in the separation of two nucleosomes is inconsistent with both the hydrodynamic and the electron microscopic results of the present study. Thus, in the absence of other forces, the bending cannot be explained by thermal fluctuations of naked DNA. It is the limited extent of these that leads to the large persistence length of naked DNA; as discussed above, this conclusion applies even to the limiting persistence length, which obtains in high [Na^+].

Presumably the bending is facilitated by proteins. It is possible that a large favorable free energy of nucleosome association simply exceeds the resistance of DNA to bending. Alternatively, H1 (or H5) or "tails" of the core histones (1) may actively bend the linker DNA, or the DNA may bend because of asymmetric charge neutralization by bound protein residues (32, 33). It is noteworthy that histone H1 is known to exhibit a significant [Na^+]-dependent structural change (34) between ≈0.0 and 0.1 M Na^+, and a [Na^+]-dependent change from noncooperative to cooperative binding to naked DNA between 20 and 40 mM Na^+ (35) [although histone H5 shows cooperative binding to naked DNA at least down to 5 mM Na^+ (36)]. It should be possible to distinguish between the different models for DNA bending by studying dinucleosomes that selectively lack H1 (or H5) or individual core histone "tails" (37).

The present results relate to two other significant aspects of the mechanism of chromatin folding. Na^+-dependent chromatin folding (i.e., chromatin folding *in vitro*) is known to be a continuous, rather than a two-state, process (2). At intermediate concentrations of Na^+, chromatin fibers have an intermediate width; the two limit states (nucleosome filament and 30-nm filament) are largely unpopulated. However, this conclusion is based on measurements that are averaged over stretches of chromatin fibers that are many nucleosomes long. It would be of great interest to determine whether folding is continuous or two-state at the level of individual pairs of nucleosomes. Finally, it should be recognized that the present results do not constitute evidence against cooperativity in chromatin folding. A tendency of consecutive units along a chain to interact does not preclude the existence of additional forces, such as those that in helix–coil transition theory lead to cooperative behavior. Changes in the stoichiometry of histone H1 or enzymatic modification of any of the histones are means by which cooperative interactions could be modulated.

Electron microscopes were provided by the University of Illinois Center for Microanalysis of Materials. We thank R. B. Gennis, J. O. Thomas, K. E. van Holde, A. H.-J. Wang, and P. G. Wolynes for comments on the manuscript. J.W. acknowledges research support from the National Institutes of Health, the Searle Scholars Program of the Chicago Community Trust, and a National Science Foundation Presidential Young Investigator Award, and the generous donation of equipment by Apollo Computer.

1. van Holde, K. E. (1989) *Chromatin* (Springer, Berlin).
2. Widom, J. (1989) *Annu. Rev. Biophys. Biophys. Chem.* **18,** 365–395.
3. Finch, J. T. & Klug, A. (1976) *Proc. Natl. Acad. Sci. USA* **73,** 1897–1901.
4. Thoma, F., Koller, Th. & Klug, A. (1979) *J. Cell Biol.* **83,** 403–427.
5. Widom, J. & Klug, A. (1985) *Cell* **43,** 207–213.
6. Hagerman, P. J. (1988) *Annu. Rev. Biophys. Biophys. Chem.* **17,** 265–286.
7. Hagerman, P. J. (1981) *Biopolymers* **20,** 1503–1535.
8. Bordas, J., Perez-Grau, L., Koch, M. H. J., Vega, M. C. & Nave, C. (1986) *Eur. Biophys. J.* **13,** 157–173.
9. Williams, S. P., Athey, B. D., Muglia, L. J., Schappe, R. S., Gough, A. H. & Langmore, J. P. (1986) *Biophys. J.* **49,** 233–248.
10. Smith, M. F., Athey, B. D., Williams, S. P. & Langmore, J. P. (1990) *J. Cell Biol.* **110,** 245–254.
11. Widom, J. (1986) *J. Mol. Biol.* **190,** 411–424.
12. Butler, P. J. G. & Thomas, J. O. (1980) *J. Mol. Biol.* **140,** 525–529.
13. Sogo, J. M. & Thoma, F. (1989) *Methods Enzymol.* **170,** 142–165.
14. Varshavsky, A. J., Bakayev, V. V. & Georgiev, G. P. (1976) *Nucleic Acids Res.* **3,** 477–492.
15. Thomas, J. O. & Rees, C. (1983) *Eur. J. Biochem.* **134,** 109–115.
16. Bates, D. L. & Thomas, J. O. (1981) *Nucleic Acids Res.* **9,** 5883–5894.
17. Bloomfield, V. A. (1985) in *Dynamic Light Scattering,* ed. Pecora, R. (Plenum, New York), pp. 363–416.
18. Libertini, L. J. & Small, E. W. (1980) *Nucleic Acids Res.* **8,** 3517–3534.
19. Burch, J. B. E. & Martinson, H. G. (1980) *Nucleic Acids Res.* **8,** 4969–4987.
20. Osipova, T. N., Pospelov, V. A., Svetlikova, S. B. & Voro'bev, V. I. (1980) *Eur. J. Biochem.* **113,** 183–188.
21. Marion, C., Bezot, P., Hesse-Bezot, C., Roux, B. & Bernengo, J. C. (1981) *Eur. J. Biochem.* **120,** 169–176.
22. Bates, D. L., Butler, P. J. G., Pearson, E. C. & Thomas, J. O. (1981) *Eur. J. Biochem.* **119,** 469–476.
23. Hirai, M., Niimura, N., Zama, M., Mita, K., Ichimura, S., Tokunaga, F. & Ishikawa, Y. (1988) *Biochemistry* **27,** 7924–7931.
24. Schmitz, K. S. & Ramsay-Shaw, B. (1977) *Biopolymers* **16,** 2619–2633.
25. Olins, A. L., Carlson, R. D., Wright, E. B. & Olins, D. E. (1976) *Nucleic Acids Res.* **3,** 3271–3291.
26. Wittig, B. & Wittig, S. (1977) *Nucleic Acids Res.* **4,** 3901–3917.
27. Gordon, V. C., Knobler, C. M., Olins, D. E. & Schumaker, V. N. (1978) *Proc. Natl. Acad. Sci. USA* **75,** 660–663.
28. Cantor, C. R. & Schimmel, P. R. (1980) *Biophysical Chemistry* (Freeman, New York), Vol. 2.
29. Richmond, T. J., Finch, J. T., Rushton, B., Rhodes, D. & Klug, A. (1984) *Nature (London)* **311,** 532–537.
30. Finch, J. T., Noll, M. & Kornberg, R. D. (1975) *Proc. Natl. Acad. Sci. USA* **72,** 3320–3322.
31. Satchwell, S. C. & Travers, A. A. (1989) *EMBO J.* **8,** 229–238.
32. Belmont, A. & Nicolini, C. (1981) *J. Theor. Biol.* **90,** 169–179.
33. Manning, G. S. (1989) *J. Biomol. Struct. Dyn.* **7,** 41–61.
34. Smerdon, M. J. & Isenberg, I. (1976) *Biochemistry* **15,** 4233–4242.
35. Renz, M. & Day, A. L. (1976) *Biochemistry* **15,** 3220–3228.
36. Clark, D. J. & Thomas, J. O. (1988) *Eur. J. Biochem.* **178,** 225–233.
37. Ausio, J., Dong, F. & van Holde, K. E. (1989) *J. Mol. Biol.* **206,** 451–463.